

ÉCOLE POLYTECHNIQUE DE LOUVAIN

---

**LELEC2910**

**Propagation Project**

---

**Delait Louis - 43341700**

May 15, 2021

## Contents

<b>1</b>	<b>Introduction</b>	<b>2</b>
<b>2</b>	<b>Objectives</b>	<b>2</b>
<b>3</b>	<b>LEO transmission Model</b>	<b>3</b>
3.1	Model Description . . . . .	3
3.2	Probability of Elevation angle . . . . .	4
<b>4</b>	<b>Attenuation Effects</b>	<b>5</b>
4.1	Gases Attenuation . . . . .	5
4.2	Rain Attenuation . . . . .	7
4.3	Cloud Attenuation . . . . .	10
4.4	Scintillation Attenuation . . . . .	12
4.5	Total Attenuation . . . . .	13
<b>5</b>	<b>Link Budget</b>	<b>15</b>
5.1	Transmission chain equation . . . . .	15
5.2	Receiving antenna gain . . . . .	15
5.3	Path losses . . . . .	16
5.4	Noise . . . . .	17
5.5	SNR . . . . .	17
5.6	EIRP Computation . . . . .	17
<b>6</b>	<b>Conclusion</b>	<b>19</b>

## 1 Introduction

The European Space Agency (ESA) has launched a project for the design, fabrication and launch of a W-band Cubesat at 76 GHz.

Eventhough the data throughput increases at 75 GHz, the degradation due to gases, rain, and clouds becomes important at this range of frequency. Therefore, available propagation-models are not accurate up 50 GHz.

Furthermore the Cubesat follows a non-geostationary orbit and there are nearly no propagation measurements available for this kind of orbital revolution.

This project aims to determine the effect of the troposphere on wireless transmissions with LEO satellites at such frequencies and then to compute a link budget of the transmission. In order to increase the accuracy of the model, we will discuss of the transmission at a second frequency of 37.5 GHz.

## 2 Objectives

The main goals of this project are :

1. Model and analyse **the attenuation due to propagation through the troposphere** and the importance of the different attenuation causes based on the RAPIDS II version Pastel propagation tool.
2. Compute a **link budget** for the transmission at both frequencies assuming different time percentage availability.

This study will be lead for 2 transmitting antennas that are located as followed :

	Latitude (°)	Longitude (°)	altitude [m]
Graz (Austria)	47.07N	15.44E	353
Isfjord (Norway)	78.05N	13.6E	7



Figure 1: base stations locations

### 3 LEO transmission Model

#### 3.1 Model Description

The available software RAPIDS II only allows to get data on attenuation for fixed position of the receiver (Geostationary Satellites). We thus have to take some assumptions in order to model attenuation due to propagation for transmission with LEO (Low Earth Orbit) satellites.

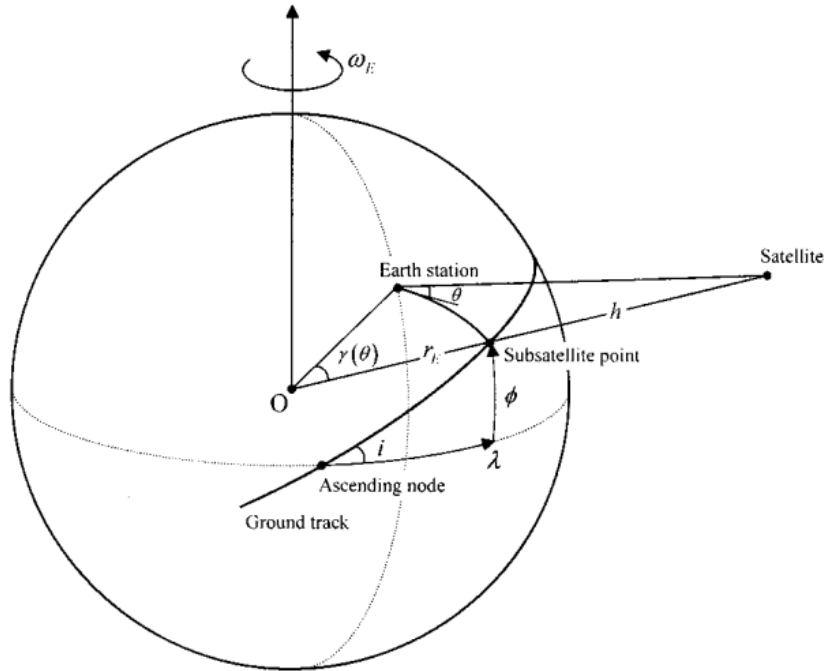


Figure 2: Earth-Satellite positioning  
from Reference (2)

In the point of vue of the antenna on the ground, a LEO satellite rises at one point of the horizon, crosses the sky and sets at the opposite point in the horizon.

We will compute the tropospherical attenuation due to transmission with LEO satellite based on the method developed in R-REC-P.618 (1) : Taking the attenuation for discrete elevation angles for transmission with GEO satellites and computing a weighted average of this attenuations. The weights depending of the percentage of the visible time the satellite spends at this elevation angle; such that the lower is the elevation angle, the higher is the probability of seeing the LEO satellite (see figure 2). For the rest of this report, we will assume the following probability distribution for the elevation angles (based on discussion in section 3.2):

$\theta [^\circ]$	5	15	25	35	45	55	65	75	85
Probability [/]	0.2967	0.2011	0.1359	0.0961	0.0723	0.0579	0.0492	0.0442	0.0419

Thus the total tropospherical attenuation is computed by taking a weighted average of the attenuation due to the considered elevation angle. This will be done in section 4.5.

### 3.2 Probability of Elevation angle

Based on the reference (2), the probability density function (pdf) of elevation angles for a single satellite can be expressed as

$$f(\theta) = \frac{G(\theta)\sin(\gamma(\theta))}{\sqrt{\cos^2(\gamma_{\theta max}) - \cos^2(\gamma_{\theta max})} \cdot \arccos\left(\frac{\cos(\gamma_{\theta min})}{\cos(\gamma_{\theta max})}\right)} \quad (1)$$

with  $\gamma$  and  $\theta$  as defined in the figure (2),

$$\begin{aligned} a &= \frac{R_{\text{earth}}}{R_{\text{earth}} + \text{Altitude}} \\ \gamma &= \arccos(a \cos(\theta) - \theta) \\ G(\theta) &= \frac{1 + a^2 - 2a \cos(\gamma(\theta))}{1 - a \cos(\gamma(\theta))} \end{aligned}$$

Without more information about the orbit of the satellites used in this project, the assumption is made that the satellite at its zenith is above the base station. In other words, that  $\theta \in [0; \pi/2]$  and then  $\gamma_{\theta min} = \arccos(a)$  and  $\gamma_{\theta max} = 0$ . We also take  $R_{\text{earth}} = 6371[\text{km}]$  and  $\text{Altitude} = 817[\text{km}]$  from project data.

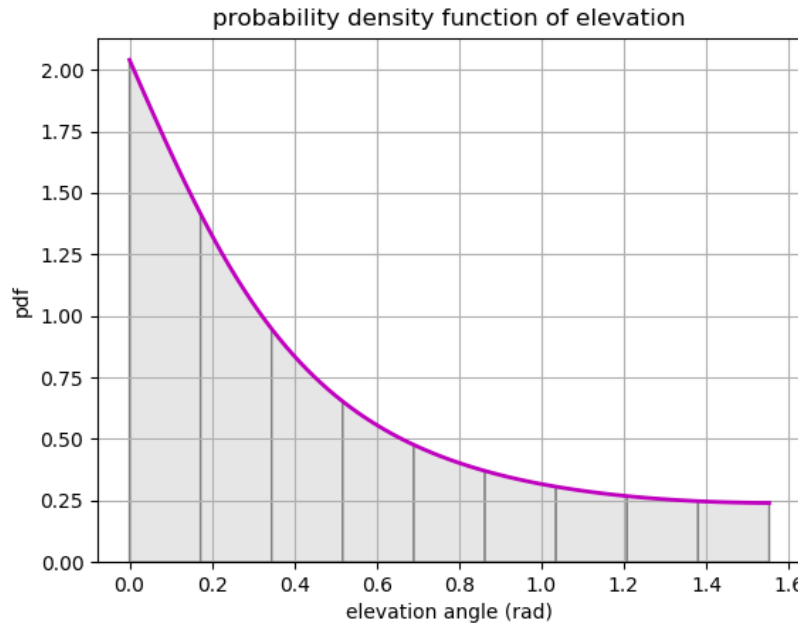


Figure 3: Probability associated to elevation angles

It is then possible to get the probability associated to a certain range of elevation angles by integrating this probability density function on this range of angles. Separating into 10 degree increments the abscissa domain (See figure 3), we get this probability distribution :

$\theta [\text{°}]$	[0,10[	[10,20[	[20,30[	[30,40[	[40,50[	[50,60[	[60,70[	[70,80[	[80,90[
Probability [%]	0.2967	0.2011	0.1359	0.0961	0.0723	0.0579	0.0492	0.0442	0.0419

### Remark about this model

Taking into account that the elevation angle  $\theta \in [0; \pi/2]$  is a big assumption and all the following results will depend on it. As the MetOp satellites used here are Polar-orbiting satellites, the maximum elevation angle pointed by the ground station changes at each revolution (See figure 4). Thus the case that we consider here is the most accommodating one, as the farther away the satellite's ground track is from the station, the less  $\theta_{max}$  will get close to 90°, and then the highest the weighted average of the attenuation due to troposphere will be, as the attenuation mainly decreases with elevation angle. It is however easy to compute results for different ranges of reachable elevation angles following the reasoning of this report : By computing for each revolution the probability distribution of elevation angle and then recomputing the weighted average to get total attenuation and needed EIRP.

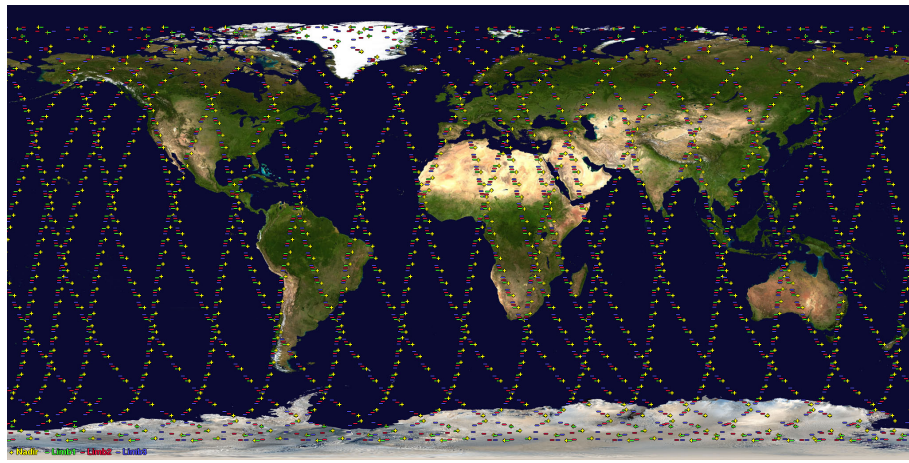


Figure 4: Ground Track of a 700 km high Polar-orbiting satellite  
from Reference (7)

## 4 Attenuation Effects

In this section we will discuss the attenuation level due to the following components :

- Rain
- Clouds
- Gases
- Scintillation

Then compute the total attenuation and discuss the importance of each component for the stations located in Graz and Isfjord.

### 4.1 Gases Attenuation

The gaseous attenuation is mainly due to dipolar or ionic polarisation that appears into damped oscillations and alignment or resonant effects.

The losses can be modeled mathematically by introducing the complex permittivity of the medium  $\epsilon = \epsilon' - j\epsilon''$ . The imaginary part implies losses in the medium and a  $\sigma_{eq} \neq 0$  (although the conductivity  $\sigma = 0$ ) by the relation

$$\epsilon'' = \frac{\sigma_{eq}}{\omega}$$

The gaseous attenuation is then frequency dependent. Talking in terms of refractivity rather than in terms of permittivity, the main compounds of radio refractivity are due to oxygen and water vapor.

The total refractivity can be expressed as

$$N_{tot} = \underbrace{N_0}_1 + \underbrace{N_o(f)}_2 + \underbrace{N_n(f)}_3 + \underbrace{N_V(f)}_4 + \underbrace{N_C(f)}_5 \quad (2)$$

With

1.  $N_0$  the non-dispersive term due to contributions of oxygen, water vapor and liquid or ice water.
2.  $N_o(f)$  the term due to resonance of oxygen particules.
3.  $N_n(f)$  the non-resonant oxygen term..
4.  $N_V(f)$  the term due to line spectra of water vapor.
5.  $N_C(f)$  the term relative to water vapor continuum.

Developing all this terms we finally get a specific attenuation

$$\gamma_a(\vec{r}, f) = 0.1820 \cdot f \cdot N(f) \quad [dB/km] \quad (3)$$

We then can find the total attenuation by integrating the specific attenuation on the path :

$$A_g = \int_h^\infty \frac{\gamma_a(\vec{r}, f)}{\sin(\Phi(z))} dz \quad [dB] \quad (4)$$

$h$  being the altitude and the sinus coming from the ray bending effect: for low elevation angles the wave is subject to a phenomenon of multiple refraction.

Using the software RAPIDS II, we get the attenuation due to gases as a function of the the elevation angle (see figures (5) and (6)).

The shape of the simulation curves confirms to previously introduced model (Eq 3) as the attenuation increases with the frequency for both oxygen and water vapor.

Furthermore we observe that the attenuation due ton oxygen is higher both at 75 [GHz] and 37.5 [GHz]. We can assume that it is due to the first resonance frequency of the dioxygen ( $\approx 60$ [GHz]) that is close from both carrier frequency. For comparison the first or second resonance frequency of the water vapor are respectively  $\approx 20$ [GHz] and  $\approx 183.3$ [GHz]. We can then assume that more energy is absorbed by the dioxygen molecules at this frequencies.

Finally, the attenuation level increases with the elevation angle in all the cases because the lower is  $\theta$ , the higher is the layer to cross towards the satellite.

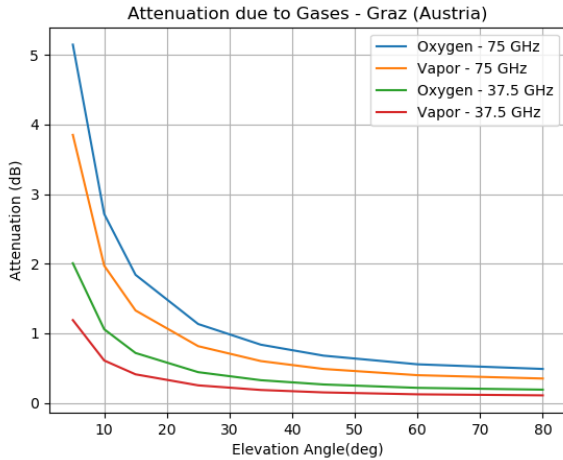


Figure 5: Attenuation due to gases (Graz)

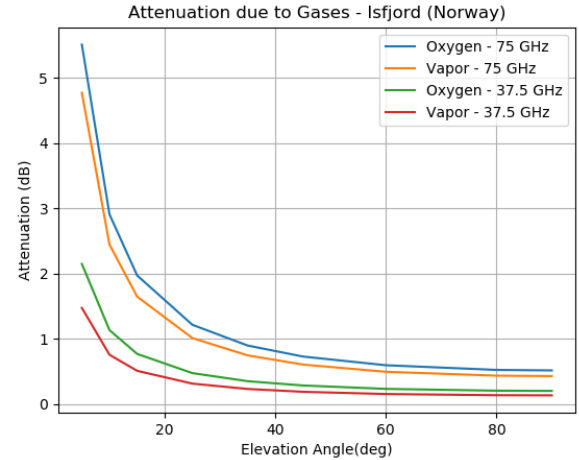


Figure 6: Attenuation due to gases (Isfjord)

## 4.2 Rain Attenuation

The raindrop attenuation is mainly due to absorption (Energy radiated in the form of heat) and scattering. The extinction is defined as the sum of this 2 effects and is the total attenuation in the forward direction due to rain.

For single-particle scattering, the scattered electric field is equal to the incident electric field multiplied by a tensor (constant in the isotropic case) called the 'scattering function'  $f(u_s, u_i)$ .

Following system parameters, we can adapt this model (and then the scattering function), 'a' being the mean drop diameter :

- **Mie Theory** : for small range of frequencies (under  $f \approx 100[\text{GHz}]$ )

We can get the scattered electric field with an exact formula (implying an infinite sum). The model consider scattering of the electric field by spherical raindrops but can be expanded for non-spherical drops.

- **Rayleigh Scattering** : for  $a \ll \lambda$

We can consider the electric field inside the particle as matching with the electrostatic solution of the Maxwell's equations. The scattering function becomes directly proportional to the droplet volume.

- **Born Approximation** : for  $(\epsilon_r - 1)k_0a \ll 1$

The field inside the scatterer drop is approximated by the incident field.

- **WKB interior wavenumber Approximation** : for  $(\epsilon_r - 1)k_0a \gg 1$  and  $\epsilon_r - 1 < 1$

The field inside the scatterer drop is approximated by the field propagating in the direction of propagation of the incident field (with the wave number of the medium of the drop).

We assume we can model rain attenuation by first order multiple scattering: single-particle scattering with attenuation on the path. It is valid for low and intermediate density of particles as in the case of rain and clouds.

For a first-order multiple scattering, the attenuation is expressed by multiplying the intensity taken away from the wave with  $\sigma_{ext}(D)$ , defining  $\sigma_{ext}(D)$  as the extinction cross-section being 'the area which, when multiplied by the incident intensity in [W/m<sup>2</sup>], provides the power taken away from the incident wave' (Reference (6)).

For a slab of thickness  $dz$  and surface  $A(z) \approx A(z + dz)$ :

The power taken away from the wave can be expressed as :

$$P_d[W] = I(z) \int_0^{\infty} \sigma_{ext}(D) N(D) A(z) dz dD \quad (5)$$

The intensity of the wave :

$$I(z + dz) = I(z) + dI(z) = \frac{P_i - P_d}{A(z + dz)}$$

the term  $dI(z)$  being negative because the energy is taken away from the wave.

Then

$$\begin{aligned} \frac{dI(z)}{dz} &= -\frac{P_d}{A} = -I(z) \int_0^\infty \sigma_{ext}(D) N(D) dD \\ \Rightarrow I(z) &= I(0) \int_0^\infty \sigma_{ext}(D) N(D) dD z \end{aligned}$$

The specific attenuation due to rain  $\gamma_{rain} \propto 10 \log(\frac{I(z)}{I(0)})$  is then expressed as

$$\gamma_{rain} = 4.343 \cdot 10^{-3} \int_0^\infty \sigma_{ext}(D) N(D) dD \quad [dB/km] \quad (6)$$

With  $N(D)$  being the number of raindrop of diameter  $D$  per  $m^3$ , that is modeled by the Marshall-Palmer distribution (Reference (9)).

A way to approximate this law is via a non-linear least-squares fitting procedure by a power law relationship as

$$\gamma_{rain} \approx kR^\alpha$$

$R$  is the rainfall rate,  $k$  and  $\alpha$  are empirical parameters.

Using the software RAPIDS II, we get the attenuation due to rain as a function of the percentage of time the attenuation is exceeded with the elevation angle as a parameter for both stations (see figures (7),(8),(9) and (10)). We notice that attenuation due to raindrop increases with the frequency as suggested by the Mie model.

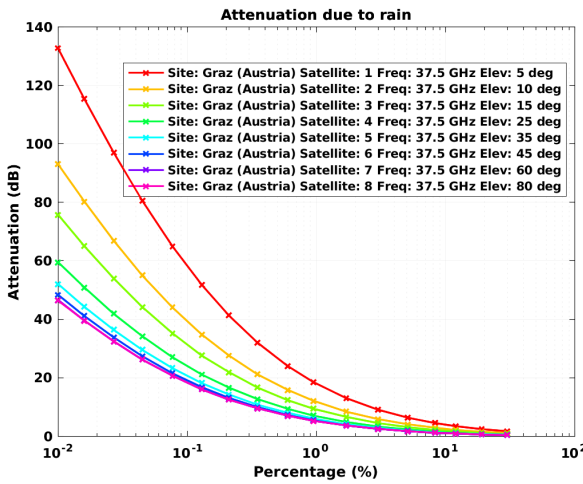


Figure 7: Attenuation as a function of the percentage of time it is exceeded (Graz -  $f_c = 37.5[GHz]$ )

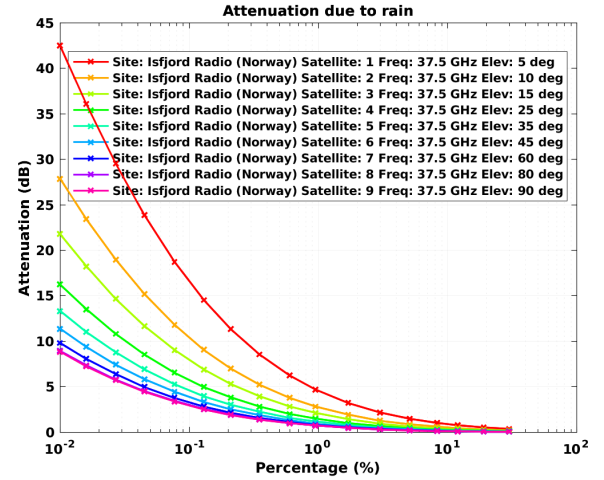


Figure 8: Attenuation as a function of the percentage of time it is exceeded (Isfjord -  $f_c = 37.5[GHz]$ )

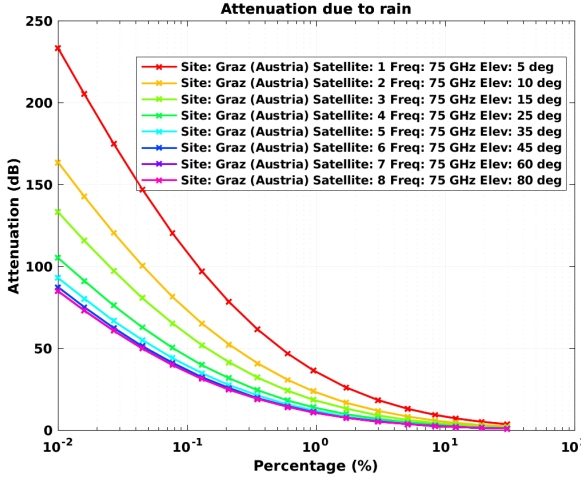


Figure 9: Attenuation as a function of the percentage of time it is exceeded (Graz -  $f_c = 75[\text{GHz}]$ )

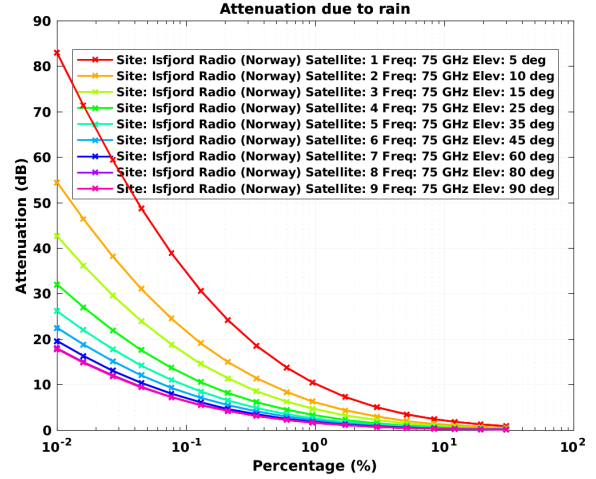


Figure 10: Attenuation as a function of the percentage of time it is exceeded (Isfjord -  $f_c = 75[\text{GHz}]$ )

We as well notice that due to climatic conditions in Austria, for low probabilities the attenuation is larger by up to 110 [dB] at 37.5 GHz and to 150 [dB] at 75 GHz compared to the attenuation in Norway. To understand this difference of level of attenuation, it is necessary to derive the rainfall rate exceeded for a given average annual probability of exceedance for both locations (using the reference (3)).

The pre-computed map of  $R_{0.01}$  can be used with insignificant loss in accuracy (See figure 11). This map gives the rainfall rate exceeded for 0.01% of an average year in [mm]. Furthermore the absolute value of the difference between the full rainfall rate prediction method, that is explained in the recommendation, and the pre-computed  $R_{0.01}$  map is less than 0.3 mm/hr for greater than 99.9% of the surface of the Earth, and the absolute value of the difference between the full rainfall rate prediction method and the  $R_{0.01}$  map is less than 1 mm/hr for greater than 99.99% of the surface of the Earth.

We can then draw some tendencies from this figure: In addition to the fact that the average annual rain fall rate is much higher in Graz than in Isfjord (respectively 873.8 mm/year and 337 mm/year), the rain fall rate in Graz exceeds 0.01 % of the time the average rain fall rate by 35 mm/hr while the rain fall rate in Isfjord exceeds 0.01 % of the time the average rain fall rate by 15 mm/hr. The rain fall rate distribution is then closer around its mean value for the station located in Isfjord, leading to a lower attenuation for low percentage of the time of availability compared to the situation in Graz.

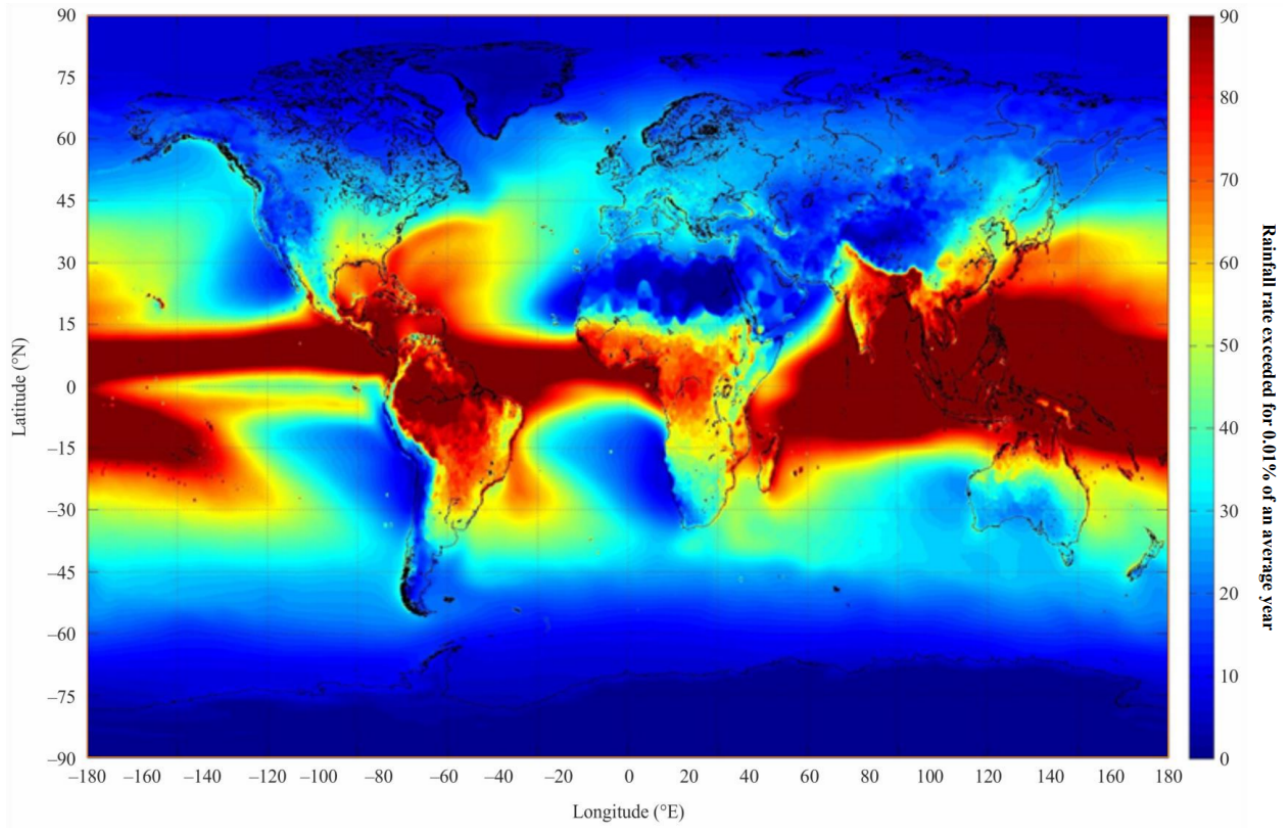


Figure 11: Rainfall rate exceeded for 0.01% of an average year [mm]

### 4.3 Cloud Attenuation

For cloud droplets, the Rayleigh approximation is valid for both carrier frequencies. The scattering function  $f(u_s, u_i)$  is then directly proportional to the droplet volume according to Rayleigh approximation.

Based on the rain attenuation theory: As the extinction cross section is proportional to the scattering amplitude, we can write the expression of the specific attenuation due to clouds:

$$\gamma_{cloud} \propto \int_0^{\infty} D^3 N(D) dD \quad [dB/km]$$

Furthermore, knowing that the expression of the liquid water content at a certain altitude ( $w(z)[g/m^3]$ ) is proportional to the same quantity :

$$w(z) \propto \int_0^{\infty} D^3 N(D, z) dD$$

The specific attenuation due to clouds is directly proportional to the liquid water content at a certain altitude. Finally the total attenuation due to clouds is found by integrating the specific attenuation on the path of the wireless transmission as

$$A(P) \propto \int \gamma_{cloud} \propto \int w(z) \propto L(P)$$

with P the percentage of time the attenuation is over this value and L the total liquid water content that is found by integrating the water content on all the altitudes whereby the signal passes.

The expression of the attenuation due to clouds is given by

$$A(P) = \frac{L(P)K_f}{\sin(\alpha_1)} \quad (7)$$

With  $K_f$  a coefficient defined as  $K_f = \frac{0.819f}{\epsilon''(1+\eta)}$  and the term  $\sin(\alpha_1)$  that corresponds to the impact of the elevation angle on the distance the signal crosses the cloud.

For both stations, using the software RAPIDS II, we get the attenuation due to cloud as a function of the percentage of time the attenuation is exceeded with the elevation angle as a parameter (see figures (12), (13), (14) and (15)).

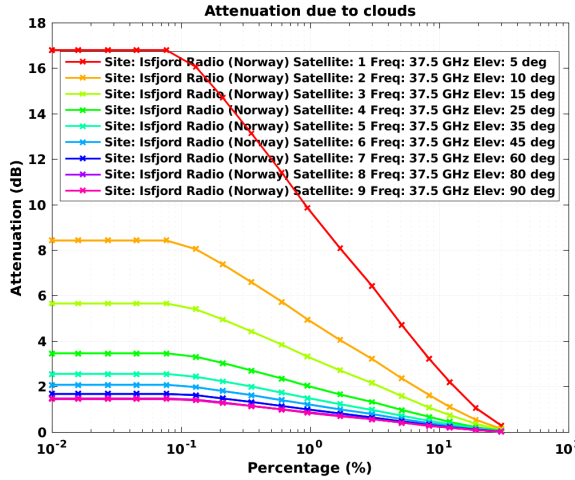


Figure 12: Attenuation as a function of the percentage of time it is exceeded (Isfjord -  $f_c = 37.5[\text{GHz}]$ )

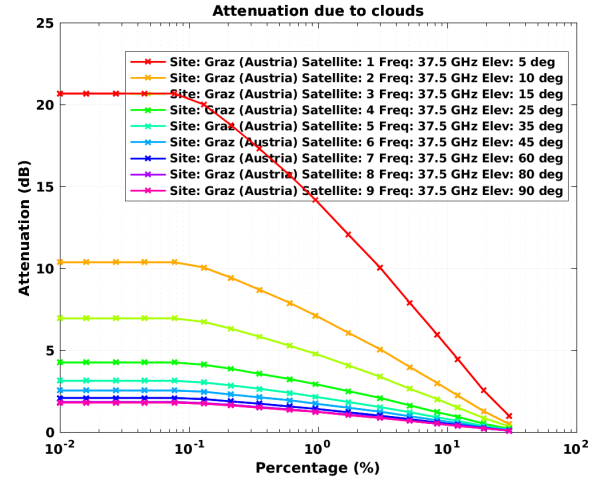


Figure 13: Attenuation as a function of the percentage of time it is exceeded (Graz -  $f_c = 37.5[\text{GHz}]$ )

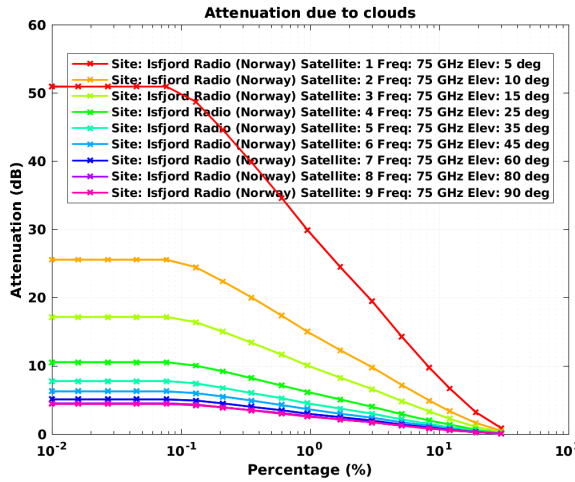


Figure 14: Attenuation as a function of the percentage of time it is exceeded (Isfjord -  $f_c = 75[\text{GHz}]$ )

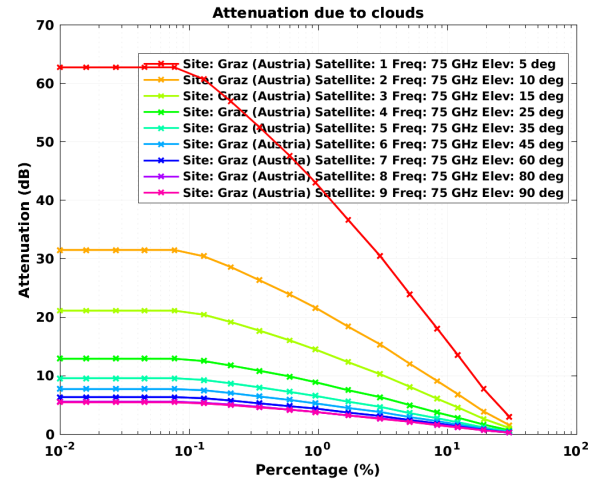


Figure 15: Attenuation as a function of the percentage of time it is exceeded (Graz -  $f_c = 75[\text{GHz}]$ )

As the total liquid water content decreases with the percentage of time, the attenuation does the same : If we want the total water content corresponding to a low percentage of time, the more we decrease this percentage, the more the total water content increases, moving away from the average total water content.

Below 0.1 %, the total liquid water content becomes constant, leading to a constant attenuation (See figure (16) and (17)). We also see on the figures (12), (13), (14) and (15) that the attenuation strongly increases with the carrier frequency as expected, seeing the frequency dependence of the factor  $K_f$  in the equation 7.

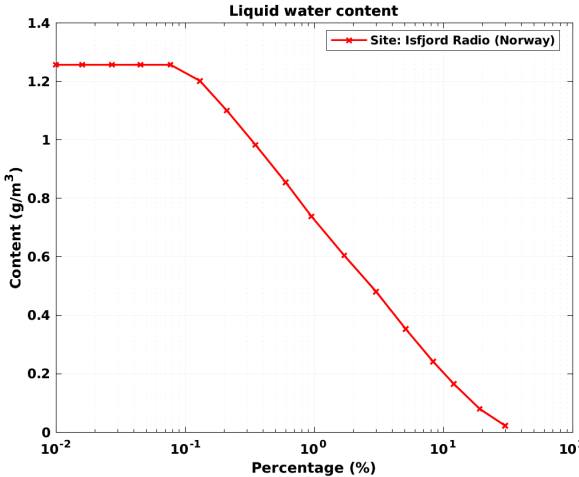


Figure 16: Isfjord

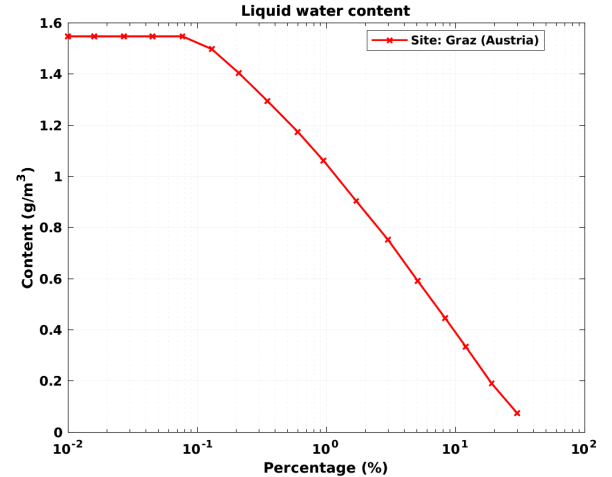


Figure 17: Graz

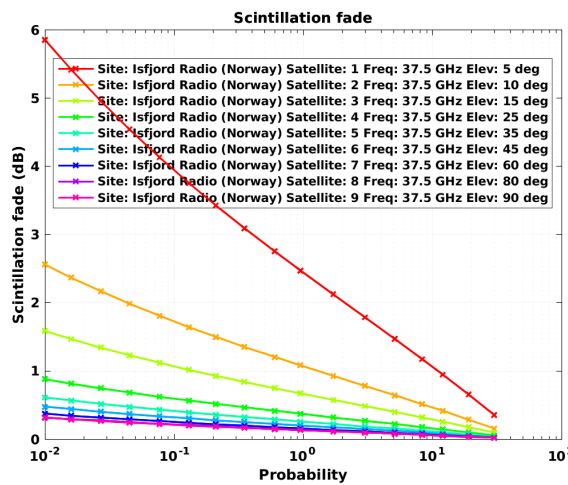
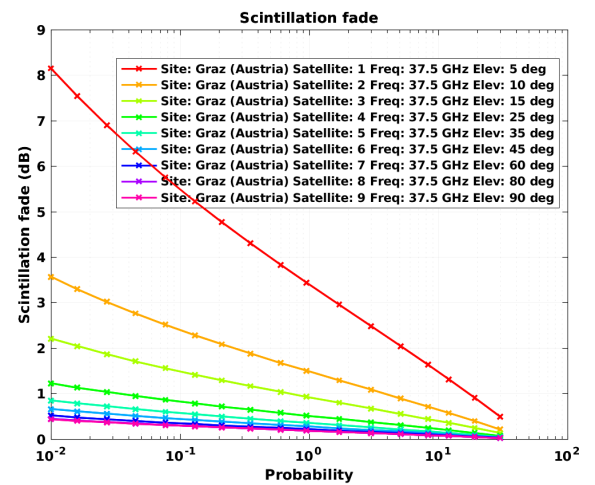
#### 4.4 Scintillation Attenuation

The scintillation is due to fast fluctuations of received signal amplitude and phase on earth-space links. It is characterised by random successive fades and enhancements associated to small-scale permittivity inhomogeneities (and then refractive-index as  $n = \sqrt{\epsilon_r}$ ) that can be caused by turbulences.

The scintillation is pretty hard to predict because it is a random variable that depends on fluid mechanics principles. It is modeled empirically based on wet part of ground refractivity (Reference (4)). It is then possible to calculate the scintillation standard deviation for link parameters

$$\sigma = \sigma_{ref} \sqrt{\frac{f^a G}{\sin^b(\theta)}}$$

Using the software RAPIDS II, we get the attenuation due to scintillation as a function of the percentage of time the attenuation is exceeded with the elevation angle as a parameter (see figures (18),(19),(20) and (21)). The attenuation increases with the decreasing elevation angle and the increasing carrier frequency as the variance increases, leading to more spread attenuation and then higher attenuation for the same percentage of time.

Figure 18: Attenuation as a function of the percentage of time it is exceeded (Isfjord -  $f_c = 37.5[\text{GHz}]$ )Figure 19: Attenuation as a function of the percentage of time it is exceeded (Graz -  $f_c = 37.5[\text{GHz}]$ )

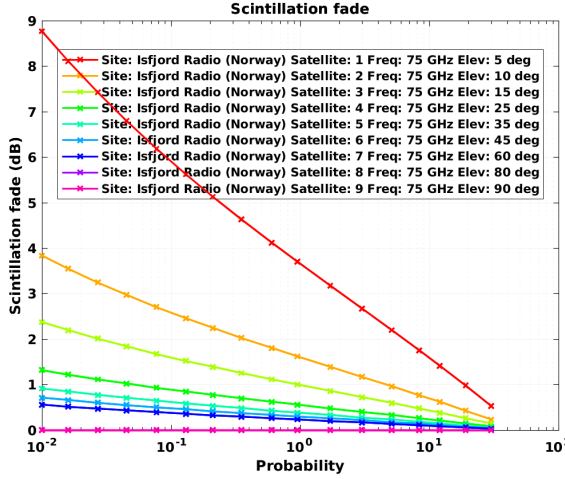


Figure 20: Attenuation as a function of the percentage of time it is exceeded (Isfjord -  $f_c = 75[\text{GHz}]$ )

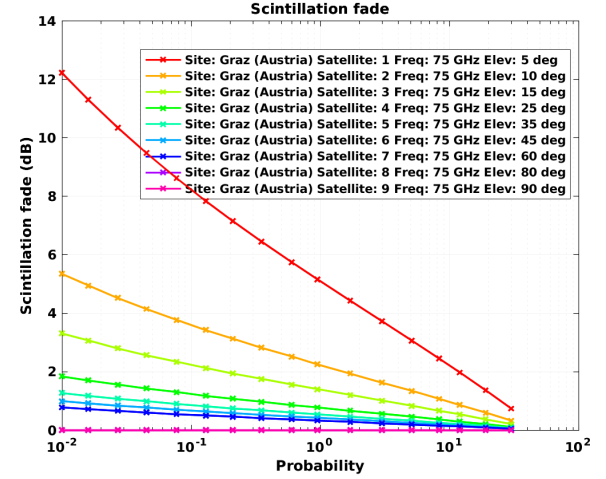


Figure 21: Attenuation as a function of the percentage of time it is exceeded (Graz -  $f_c = 75[\text{GHz}]$ )

#### 4.5 Total Attenuation

The total attenuation takes into account the rain, clouds, gases and the scintillation. Computing a weighted average (following the reasoning at section 3.1) on all the possible elevations, the following curves are obtained (figures (22), (23), (24) and (25)). The comparative order of importance of each component in the total attenuation on this graph is characteristic for a wireless transmission through the troposphere.

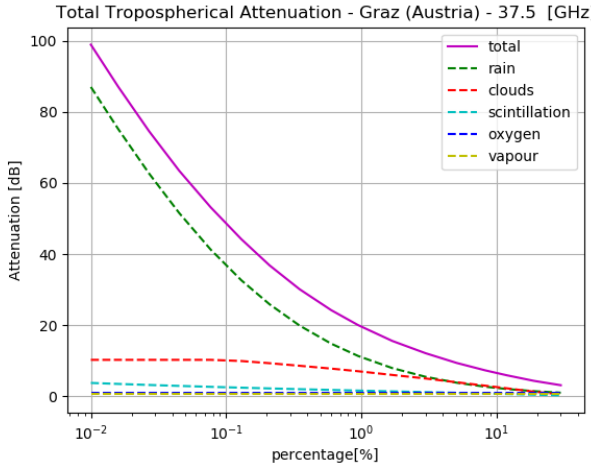


Figure 22: Total attenuation and all its components (Graz - 37.5 [GHz])

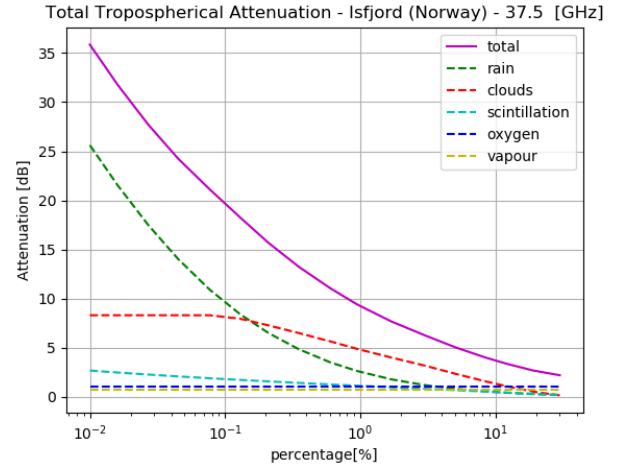


Figure 23: Total attenuation and all its components (Isfjord - 37.5 [GHz])

We see on the figures (22), (23), (24) and (25) that the rain attenuation dominates the total attenuation followed by the cloud attenuation, the scintillation, the oxygen and then the water vapor attenuation for both locations. The comparative difference of attenuation due to rain leads to a much higher total attenuation for the transmission with the antenna located in Graz. This effect has been analysed in previous sections. Based on the model introduced in section 3.1, we get the following curves for the average total attenuation for both the station located in Norway and Austria, at 37.5 and 75 [GHz] for a transmission with LEO satellite (figures (26) and (27)). The main impact of the increasing carrier frequency is more attenuation due to troposphere.

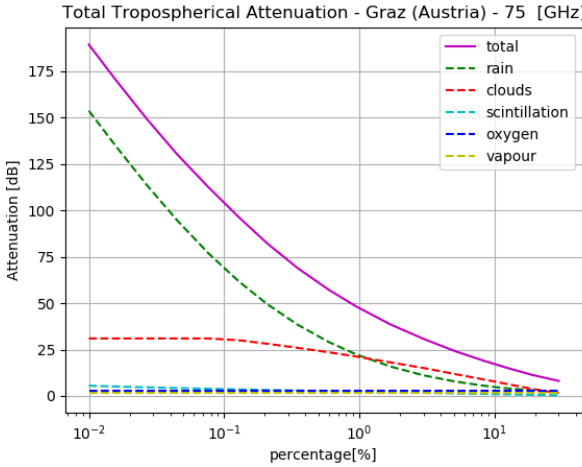


Figure 24: Total attenuation and all its components (Graz - 75 [GHz])

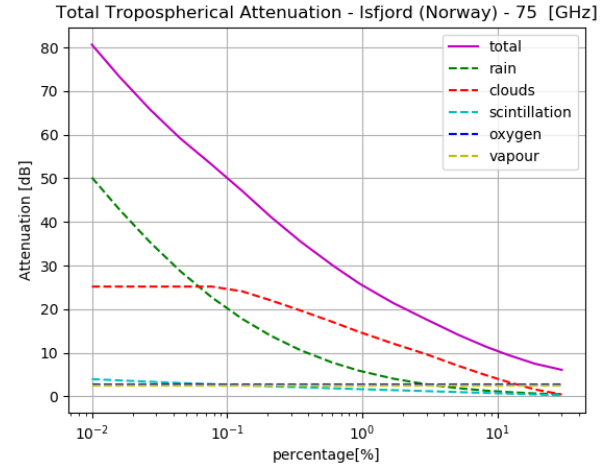


Figure 25: Total attenuation and all its components (Isfjord - 75 [GHz])

The abscissa can be interpreted as the percentage of time the attenuation is exceeded. For example taking the attenuation at 1% means that 1% of the time the attenuation is over this value and 99% of the time it is below.

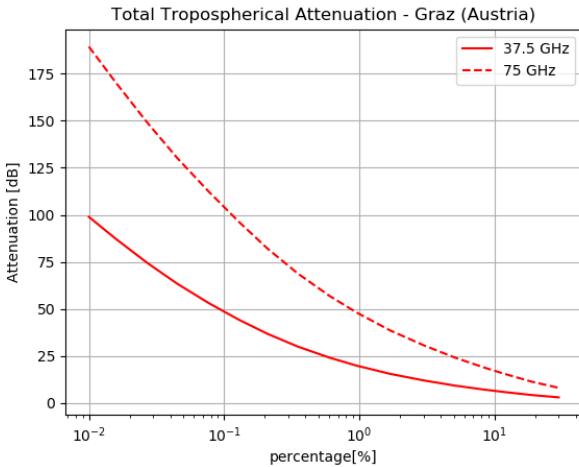


Figure 26: Attenuation as a function of the percentage of time it is exceeded (Austria)

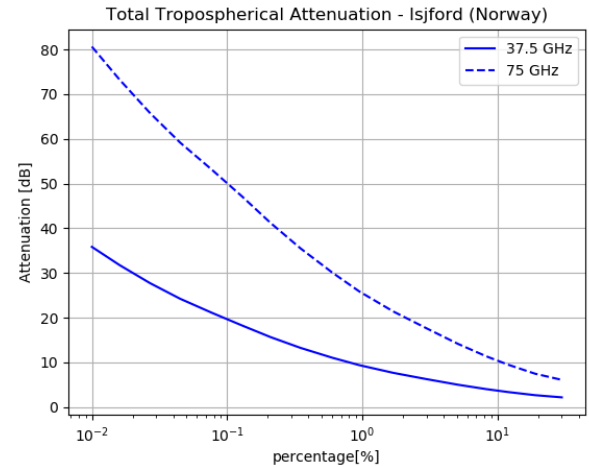


Figure 27: Attenuation as a function of the percentage of time it is exceeded (Norway)

Then knowing at which frequency we want to transmit, from which position and for what percentage of the time, we get the value of the attenuation due to troposphere for the computation of the link budget.

Availability [%]	Attenuation [dB]			
	Austria - 37.5 [GHz]	Austria - 75 [GHz]	Norway - 37.5 [GHz]	Norway - 75 [GHz]
99	20.5	28.7	9.8	26.1
99.5	48.6	61.6	13.4	33.3
99.9	49.7	108.0	19.9	50.1
99.99	99.8	183.2	36.6	80.4

## 5 Link Budget

The link budget consists in a quantification of all the power parameters of the wireless transmission.

The purpose of this section is to determine the Effective Isotropic Radiated Power (EIRP) needed at the transmitter to allow a SNR higher than 10[dB] for the whole transmission chain for different values of transmitter availability, knowing the effect of the troposphere thanks to the previous section.

### 5.1 Transmission chain equation

The equation that models the transmission chain is as followed:

$$P_R = \frac{P_T G_T G_R}{L L_T L_R} \quad (8)$$

With

- $P_R$  the received power
- $P_T$  the transmitted power
- $G_T$  the gain of the antenna at the emitting stage
- $G_R$  the gain of the receiving antenna
- $L$  the path losses, containing the tropospherical attenuation and the free space losses.
- $L_T$  the feeder losses in the transmitter
- $L_R$  the feeder losses in the receiver

As we do not have any information about the polarization and impedance mismatch in the receiver and transmitter, we assume that they are equal to 0[dB].

Furthermore the Effective Isotropic Radiated Power (EIRP) (power that leaves the transmitting antenna) can be expressed as

$$EIRP = \frac{P_T G_T}{L_T} \quad (9)$$

### 5.2 Receiving antenna gain

The gain at the receiver antenna can be expressed as

$$G_R = \frac{4 \pi A_{eff}}{\lambda^2} \quad (10)$$

with  $A_{eff}$  the effective area that is expressed by :

$$A_{eff} = \eta A \quad (11)$$

with  $A$  the area of the receiving antenna and  $\eta$  the aperture efficiency.

For the 2 carrier frequencies, the surface of the receiving antenna is the same. Knowing the transmitting antenna Gain at 75[GHz] ( $G_{R,75} = 51$  [dBi]) and using the equations (10) and (11) we get

$$G_{R,37.5} = G_{R,75} \left( \frac{\lambda_{75}}{\lambda_{37.5}} \right)^2 \frac{\eta_{37.5}}{\eta_{75}} \quad (12)$$

We then get

Carrier Frequency	37.5 [GHz]	75 [GHz]
$\lambda$ [m]	7.99E-3	3.99E-3
$\eta$ [/]	0.6	0.57
$G_R$ [dBi]	45.19	51

### 5.3 Path losses

The path losses L are composed of

- $L_{troposphere}$  : Tropospherical losses whose value have been developed in the next section for both localisation and carrier frequency.
- $L_{free-space}$  : Path losses due to the non-beam radiation of the transmitting antenna.

This section only deal with the second aspect as the first one has already be studied.

Assuming two antennas with matched polarisations, the power density arriving at the receiving antenna is (as we consider  $L_T = L_{troposphere} = 1$ )

$$S = \frac{P_T G_T}{4\pi r^2} \quad (13)$$

with r the distance between the 2 antennas.

The received power is found by multiplying this power density by the effective area of the receiving antenna :

$$P_R = \frac{P_T G_T A_{eff}}{4\pi r^2} \quad (14)$$

Combining the equations (8) and (14), we get

$$\frac{G_R}{L} = \frac{A_{eff}}{4\pi r^2}$$

Adding the equation (10), we finally get for the path losses.

$$L_{path} = \frac{(4\pi r)^2}{\lambda^2} \quad (15)$$

Finally, knowing that  $r = 2800$  [km] and assuming  $\mu_r = \epsilon_r = 1$ , we have for the 2 carrier frequencies:

Carrier Frequency	37.5 [GHz]	75 [GHz]
$\lambda$ [m]	7.99E-3	3.99E-3
$L_{path}$ [dB]	192.87	198.89

## 5.4 Noise

The noise power is due to the noise induced by the transmitting and receiving stages (antenna, amplifier, cables) and to the thermal noise that appears in the channel stages .

For this project, we consider the LNA noise temperature equal to 500 [K]. It corresponds to the noise temperature at the end of the Low Noise Amplifier, at the reception stage of the system. The noise power (N) can then be computed with the following equation:

$$N = kTB \quad (16)$$

With k the Boltzmann's constant ( $1.38064852 \cdot 10^{-23} [m^2 kg s^{-2} K^{-1}]$ ), T the LNA noise temperature and B the bandwidth used for the transmission ( $50 Hz$ ).

We then get

Carrier Frequency	37.5 [GHz]	75 [GHz]
LNA noise temperature [K]	450	500
N [dBW]	-185.08	-184.62

## 5.5 SNR

For performance evaluation the SNR (signal to noise ratio) is the most important factor and is defined as the terminology suggests by :

$$SNR = \frac{P_R}{N} = \frac{EIRP G_R}{N L} \quad (17)$$

$$SNR [dB] = EIRP [dBW] + G_R [dBi] - L_{path} [dB] - L_{troposphere} [dB] - N [dBW] \quad (18)$$

It is specified for this project that the SNR must be higher than 10 [dB] to allow detection by the receiver.

## 5.6 EIRP Computation

The purpose of this section is to get the value of the power on-board the satellite (EIRP) for the different parameters:

- Both receiving stations (Graz and Isfjord)
- Carrier frequencies of 37.5 [GHz] and 75 [GHz]
- Temporal availability of the transmitter-receiver link of 99.0, 99.5, 99.9 and 99.99%

Isolating the EIRP in equation (18) :

$$EIRP [dBW] = SNR [dB] + L_{path} [dB] + L_{troposphere} [dB] + N [dBW] - G_R [dBi] \quad (19)$$

With all the terms that have been developed in the previous sections.

The needed EIRP as a function of the temporal availability of the transmitter-receiver link is then given in figures (28) and (29).

The graph can be interpreted as followed : Taking the EIRP at 1% means that 99% of the time the EIRP has to be equal (or over) this value to get a SNR of at least 10 [dB].

Some remarks about those results:

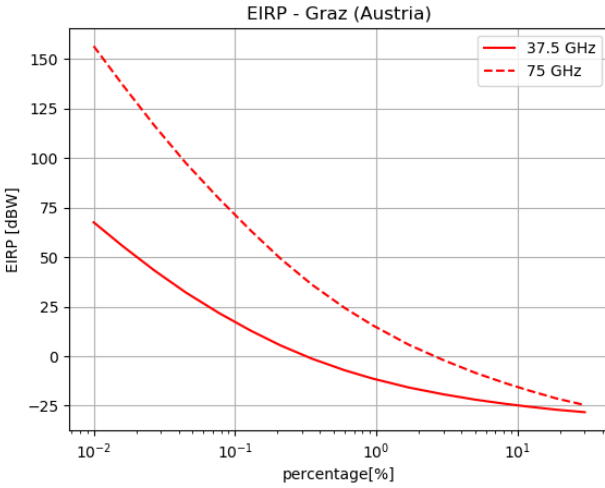


Figure 28: EIRP as a function of the percentage of time the transmission is not available - Graz

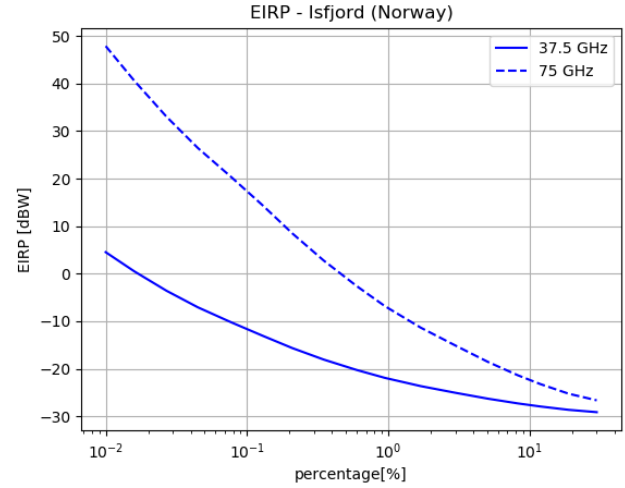


Figure 29: EIRP as a function of the percentage of time the transmission is not available - Isfjord

1. According to the previous results, as the path losses increase with the frequency of the transmission, the needed EIRP increases with the carrier frequency.
2. The higher availability we want, the higher the EIRP has to be. That is mainly due to the attenuation caused by troposphere that increases with the availability (see figures 26 and 27).
3. The needed EIRP is higher for the same carrier frequency in Austria as the tropospherical attenuation is higher in this region mainly due to climatic conditions that strongly increase the attenuation due to rain. (See section 4.2).
4. The result is an lower bound approximation as we neglected the feeder losses at the transmitter and receiver.

There are some ways to get the wanted SNR for lower power on board at the transmitter by playing with the parameters of the system:

- $G_R$  : Increasing the directivity in the direction of the transmitter can reduce the needed EIRP (as  $G_R$  will increase).
- $G_T$  : Keeping the EIRP at the level it is needed but limiting the power incoming in the transmitting antenna by increasing its directivity in the direction of the receiver.
- T : Reducing the Noise in some stages of the chain (For example the noise figure of the receiving device).

The implementation of this solutions would increase the cost of the system, maybe in a way more than the extra cost due to the lower antennas gains. However available informations about the emitting and receiving systems are missing to discuss this topic in more depth.

## 6 Conclusion

It was asked in this project to study the effect of the troposphere on wireless transmission between LEO satellites and station on earth located in Graz (Austria) and Isfjord (Norway) for different carrier frequencies. Then to compute a link budget to evaluate the needed EIRP at the transmitter to allow a SNR at detection stage of 10 [dB] for different percentage time of availability of the stations.

After having developed the way to model the LEO transmission attenuation based on the attenuation due to transmission with GEO satellites (Section 3.1), each element was studied separately (rain, clouds, gases, scintillation) and their relative importance in the total attenuation. It clearly appeared that the tropospherical attenuation is higher for the transmission at 75 [GHz] than at 37.5 [GHz] (especially attenuation due to rain and clouds) and for the transmission with the base station located in Graz, mainly due to latitude and climatic conditions that strongly increase the attenuation due to rain in this region (figures (22), (23), (24) and (25)).

Finally after a summary on the main concepts of a link budget, the EIRP was computed for each carrier frequency, percentage of time of availability and base station location. The EIRP has to be higher for the transmission at 75 [GHz] or for the transmission with the base station located in Graz, Austria (figures (28) and (29)) . This effect is mainly due to the degradation of the signal caused by the tropospherical attenuation and more particularly the attenuation due to the rain. For example the EIRP has to be higher up to 55[dBW] in Graz than in Isfjord for a percentage of availability of the transmission during the visible time of the satellite of 99.9 % at 75 [GHz].

Some important remarks about this results :

The elevation angle was considered such that  $\theta \in [0; \pi/2]$ . As the MetOp satellites used in this project are Polar-orbiting satellites, the maximum elevation angle pointed by the ground station changes at each revolution (See figure 4) . The case that we consider in this report is the most accommodating one. It is possible to compute results for different ranges of elevation angles by computing for each revolution the probability distribution of elevation angles and then computing the weighted average of attenuation and needed EIRP.

Furthermore the feeder losses  $L_T$  and  $L_R$  at the transmitter and receiver were neglected during the EIRP computation. The figures presented for the EIRP are therefore a lower limit of the real value and correspond to an ideal case.

## References

- [1] R-REC-P.618 - Section 8
- [2] Sheng-Yi Li and C. H. Liu, Fellow, IEEE.  
*An Analytical Model to Predict the Probability Density Function of Elevation Angles for LEO Satellite Systems.*  
IEEE COMMUNICATIONS LETTERS, VOL. 6, NO. 4, APRIL 2002
- [3] ITU-R P.837-7 - Annex 1
- [4] ITU-R P618-20
- [5] Claude Oestges  
*Propagation Modelling of Low Earth-Orbit Satellite Personal Communication Systems - Chapter 1.*  
December 2000
- [6] LELEC2910 - *Antennas and Propagation*
- [7] Thomas Steinholz and Andrew Davis  
*POLAR ORBITS*
- [8] eoPortal Directory  
*MetOp (Meteorological Operational Satellite Program of Europe)*
- [9] *Statistical theory of the Marshall-Palmer distribution of raindrops*